Front. Chem. China 2007, 2(1): 102–106
DOI 10.1007/s11458-007-0021-9

RESEARCH ARTICLE

ZHU Wen, YANG Junyou, GAO Xianhui, HOU Jie, BAO Siqian, FAN Xian

Preparation of bismuth telluride thin film by electrochemical atomic layer epitaxy (ECALE)

© Higher Education Press and Springer-Verlag 2007

Abstract Thin-layer electrochemical studies of the underpotential deposition (UPD) of Bi and Te on cold rolled silver substrate have been performed. The voltammetric analysis of underpotential shift demonstrates that the initial Te UPD on Bi-covered Ag and Bi UPD on Te-covered Ag fitted UPD dynamics mechanism. A thin film of bismuth telluride was formed by alternately depositing Te and Bi via an automated flow deposition system. X-ray diffraction indicated the deposits of Bi_2Te_3. Energy Dispersive X-ray Detector quantitative analysis gave a 2: 3 stoichiometric ratio of Bi to Te, which was consistent with X-ray Diffraction results. Electron probe microanalysis of the deposits showed a network structure that results from the surface defects of the cold rolled Ag substrate and the lattice mismatch between substrate and deposit.

Keywords electrochemical atomic layer epitaxy, underpotential, bismuth telluride, thermoelectric thin film

1 Introduction

Bismuth telluride belongs to the class of VA–VIA binary chalcogenide compound semiconductors with a narrow optical energy band gap of 0.13 eV and a very high figure of merit [1]. These materials are widely used for thermoelectric and optoelectronic devices, for example in solid-state refrigeration, heat pumps, subminiature electronic devices, infrared sensors, and high efficiency photovoltaic solar cells. Thin films of bismuth telluride and related compounds have already been elaborated by flash evaporation [2], co-evaporation [3], molecular beam epitaxy [4], and metal-organic chemical vapor deposition [5]. These methods are thermal and generally performed in a vacuum. Moreover, it needs expensive precursors, complicated apparatus, and produces even some toxic byproducts. Electrochemical atomic layer epitaxy (ECALE) is a technique that can be done at low-temperature and it is less costly. The methodology is the electrochemical analog of ALE; therefore, it inherits the advantages of both the electrochemical deposition and atomic layer epitaxy. ECALE involves the alternated electrochemical deposition of elements to form a compound. Epitaxial deposition is achieved by using underpotential deposition (UPD) as the means to achieve surface chemistry-limited growth. The phenomenon of UPD involves the deposition of an atomic layer of one element on a second, at a potential prior to (under) that needed to form deposits of the element on itself, namely, at the potential prior to the bulk deposition. The driving force is generally thermodynamic, involving the Gibbs energy of formation of a surface compound. ECALE cycles, involve switching deposition solutions and potentials to form each component atomic layer, it starts with exposure of the deposit to a precursor solution of the first element at its underpotential. The cell was then rinsed, a precursor solution for the second element was introduced at its underpotential, and the cell was rinsed with blank again. This process was intended to form a monolayer of the desired compound.

IIB–VIA compounds such as CdTe [8,9], CdS [10], and ZnSe [11] have been successfully formed by using ECALE, as well as IIIA–VA compound InAs [12], IIIA–VIA compound In_2Se_3 [13], IVA–VIA compound PbSe [14]. However, no work has been reported on the formation of bismuth telluride VA–VIA compound thin films by ECALE. In the present investigation, an automated computer-controlled thin-layer electrochemical flow cell system is developed in this group in order to alternate the deposition solutions to form the atomic layer of every element. Preliminary study of the ECALE process of bismuth telluride thin film and the electrochemical aspects are reported in this paper.

2 Experimental

Solutions were prepared with high purity reagents and twice-distilled water. All bismuth solutions consisted of 0.1 mmol/L

Translated from *Chinese Journal of Applied Chemistry*, 2005, 22 (11) (in Chinese)

ZHU Wen, YANG Junyou (✉), GAO Xianhui, HOU Jie, BAO Siqian, FAN Xian
State Key Laboratory of Material Processing and Die & Mould Technology, Huazhong University of Science and Technology, Wuhan 430074, China
E-mail: jyyang@public.wh.hb.cn

$Bi(NO_3)_3·5H_2O$, and using 0.1 mol/L $HClO_4$ as a supporting electrolyte, pH 1.5. Tellurium solutions were all 0.1 mmol/L in TeO_2, and also used 0.1 mol/L $HClO_4$ as a supporting electrolyte. The pH 8.5 of the Te solution was adjusted with ammonia. Various blank rinse solutions were also utilized, with a pH analogous to its respective deposition solution. All solutions were deaerated by blowing purified N_2 gas through and over the solution for 30 min. All experiments were performed at room temperature. The working electrodes were cold rolled silver (99.99%) substrates. The substrates were mirror-like polished mechanically and then annealed in a muffle furnace under a vacuum for 30 min at 650°C. Before depositions, the electrode was polished chemically for 5 s in a silver etch solution, which consisted of a mixture of 0.1 mol/L CrO_3 + 0.1 mol/L HCl. After polishing, the electrode was soaked first in concentrated ammonia for about 5 min, and then in concentrated sulfuric acid for about 20 min. Finally, it was rinsed thoroughly with water.

An automated deposition apparatus, consisting of peristaltic pumps, valves, programmable logistic computer (PLC), electrochemical flow cell, and potentiostat, was used under the control of a computer (Fig. 1). The electrolytic cavity was delimited by the working electrode and the auxiliary electrode, a plate of Pt. These electrodes were held apart by a 5-mm-thick gasket, which defined a 0.7 cm × 3 cm rectangular opening. The reference electrode, saturated calomel electrode (SCE), was positioned at the cavity outlet. At the cavity inlet, the subminiature single-directional valve bank avoided problems with mixture of solution each other via siphonal phenomena. The plexiglass was transparent, allowing the deposition process to be followed visually.

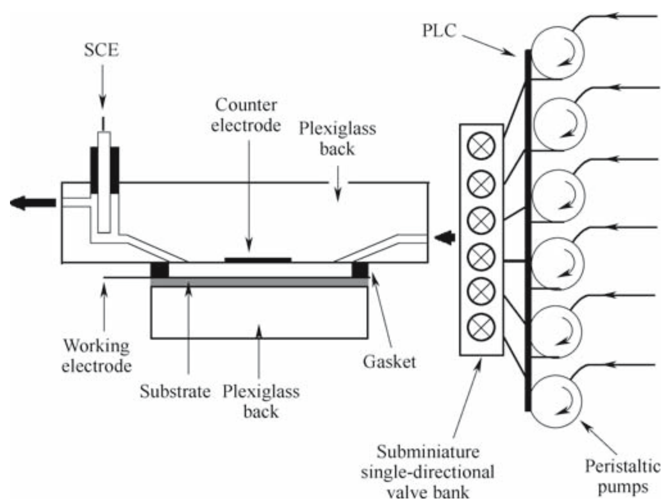

Fig. 1 The schematic drawing of an automated electrochemical thin-layer flow deposition reactor

The deposit is annealed in Ar to convert precursor layers of the elements into the compounds in 200°C. Deposit stoichiometric ratio was measured using Oxford Inca energy dispersive X-ray spectrophotometer (EDX). The XRD pattern was obtained with a Philips-PW 1710 X-ray diffractometer using CoKα radiation. Electron probe microanalysis studies were performed using a Joel JCXA-733 super probe.

3 Results and discussion

3.1 The UPD of bismuth on cold rolled Ag surface

The voltammetric profile in Fig. 2 represents the UPD of bismuth on a cold rolled silver surface. The potential in this experiment was initially scanned in the negative direction starting from a potential of 0.04 V. This potential was chosen, because it is necessary to start the deposition process with as little bismuth on the surface as possible. The quantity of precedent bismuth deposits is very little and insufficient than a single atomic layer. This deposition of a little bismuth was to prevent silver from surface oxidation, and it appeared that at least initially, the oxidation of silver was suppressed. The scan proceeded in the negative direction and resulted in a reduction peak at −0.03 V, labeled C1. The subsequent anodic stripping peaks were observed at −0.024 V and 0.08 V, labeled A2 and A1, respectively (Fig. 2(a)). Fig. 2(b) showed the corresponding increase in the cathodic electrode polarization limit. When the potential is scanned towards more negative value (−0.4 V), peak A2 increased and A1 remained unchanged. At this low concentration, there are no discernible

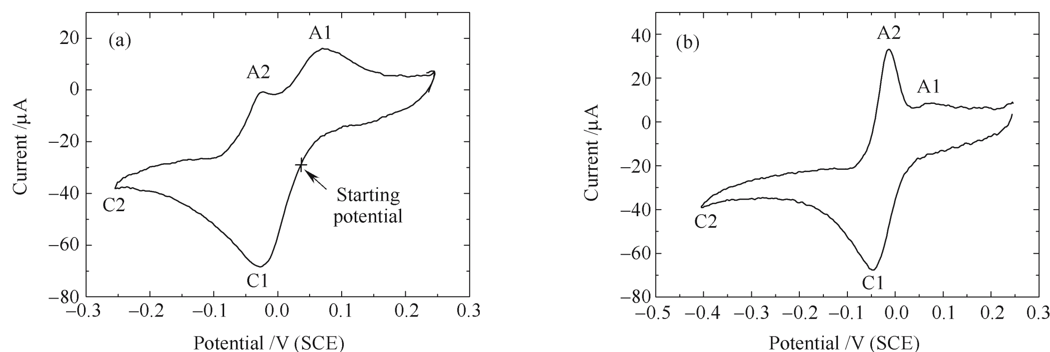

The scanning rate is 10 mV/s.

Fig. 2 Cyclic voltammogram of Bi on cold rolled silver surface starting from 0.04 V: (a) the scanning scope was from 0.25 to −0.25 V; (b) the scanning scope was from 0.25 to −0.4 V

peaks related to the bulk deposition of Bi on silver surface. In fact, increasing Bi^{3+} concentration beyond 0.4 mmol/L just causes a reduction peak at –0.4 V, so we labeled C2 at the position. Concentration dependent growth examination also showed that peak C1 and A1 were independent on Bi ion concentration, whereas peak C2 and A2 was considerably dependent on concentration. Because UPD has the characteristic of independent on ion concentration [15], this suggested that peak C1 and A1 were corresponding to UPD Bi deposition and stripping respectively while peak C2 and A2 were corresponding to bulk Bi deposition and striping.

Figure 3 shows that in the silver surface, oxidation and reduction occurred during potential cycling of Bi on the naked silver surface without the precedent Bi coverage. As shown in Fig. 3, both the silver oxidation peak and the reduction peak appear at the more positive potential as compared with the Bi UPD oxidation–reduction peaks. The resulting voltammogram (Fig. 3) is noticeably different from the voltammetry at the electrode surface without silver oxide film. Briefly, this is a negative shift (by approximately 70 mV) in Bi deposition potential (labeled C1) as compared with C1 in Fig. 2(a). Anodic stripping peak A1 is broader and shifted to a more negative potential, resulting in the overlapping of the bulk and UPD stripping peak. It is believed that the presence of the oxide layer inhibits the deposition of Bi, thus leading to the observed potential shift. In such a case, the deposition of Bi is precluded until the onset of silver oxide reduction at 0.07 V, yielding bare silver surface sites on which Bi deposition may occur.

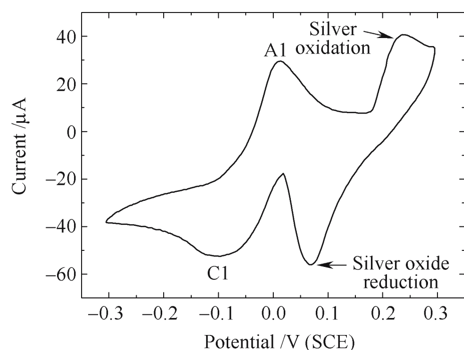

The scanning rate is 10 mV/s.

Fig. 3 Cyclic voltammogram of Bi on silver surface with silver oxide film

3.2 The UPD of tellurium on cold rolled Ag surface

The cyclic voltammogram of Te on cold rolled silver was shown in Fig. 4. The scan proceeded from –0.1 to –0.7 V and resulted in a reduction peak at –0.37 V, labeled C1, which is only observed during the first potential scan. The UPD nature of peak C1 is also supported by the fact that it disappears in the successive scannings, in which only bulk TeO_2 reduction is observed. This is in agreement with the result in the Cd–Te system on Ag (111) reported by Foresti work group [15]. Our research shows that the kinetics for Te deposition is slowed even more as solutions become more basic. In early studies, this problem was circumvented by using what is referred to here as "oxidative UPD". Oxidative UPD of Te was first put forward by Flowers et al. on the formation of a CdTe compound via the route of ECALE [8].

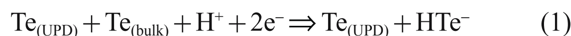

$$Te_{(UPD)} + Te_{(bulk)} + H^+ + 2e^- \Rightarrow Te_{(UPD)} + HTe^- \quad (1)$$

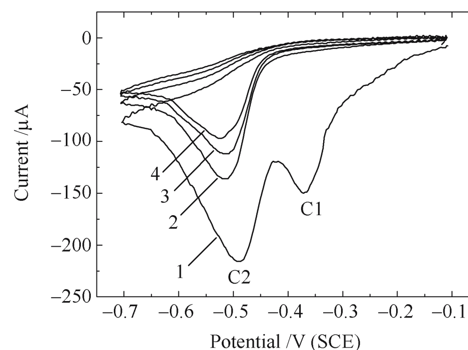

The numeral indicates consecutive scans. The scanning rate is 10 mV/s.

Fig. 4 Cyclic voltammograms of 0.1 mmol/L TeO_2 in an ammonia buffer solution of pH 8.5 on cold rolled Ag surfaces

In that program a little bulk Te and UPD Te were first deposited on the substrate. The $HTeO2^+$ solution was then exchanged for a blank electrolyte solution, and a potential sufficiently negative to reduce Te (bulk), but not negative enough to reduce Te (UPD), and Te (UPD) is left. The results show that the potential of the bulk Te reduced to HTe^- was −1.4 V, and the polarized time is 5 s.

3.3 The UPD of bismuth on Te-covered Ag surface

The cyclic voltammogram of Bi at the Te-covered Ag surface is quite different from the voltammetry at the bare Ag surface. Briefly, an initial peak, labeled C1 in Fig. 5, occurs at about –0.1 V, is shifted by about 70 mV to a less positive potential compared with bare Ag. Anodic stripping peaks A1 and A2 have a shift of 20 mV and 30 mV to a more positive potential respectively compared with the voltammogram of Bi on

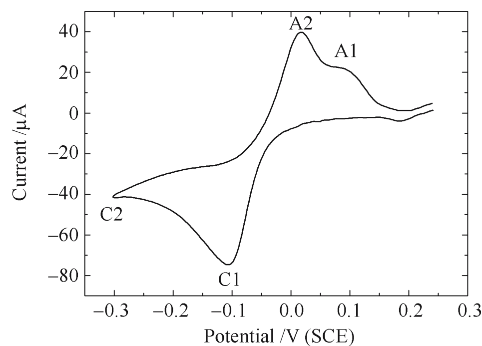

The scanning rate is 10 mV/s.

Fig. 5 Cyclic voltammogram of Bi on Te-covered cold rolled silver surface

bare Ag (Fig. 2). The underpotential shift, ΔE_p, the difference between the UPD potential and bulk deposition potential, is smaller for C1 on Te-covered Ag than on bare Ag. The underpotential shift ΔE_p, is related to the difference, $\Delta \phi$, between the work function of the depositing metal and that of the substrate. Therefore, interactions of Bi with the substrate weaker than that with the adsorbed Te atoms could shift the UPD towards more negative potential. For the same reason, the shift of anodic stripping peaks towards more positive potentials must be caused by the interaction of Bi atoms with the adsorbed Te atoms, which is obviously stronger than that with the substrate atoms and makes the Bi deposit more stable.

3.4 The UPD of tellurium on Bi-covered Ag surface

The cyclic voltammogram of Te at the Bi-covered Ag surface is shown in Fig. 6. In comparison with Fig. 4, the Te UPD peak has not been observed. However, the Te bulk deposition peak C2 is obviously stronger than that on bare Ag substrate. This means that the presence of bismuth somehow hinders Te deposition. In other words, the interactions of Te with the substrate, which are responsible for the underpotential deposition, become weaker in the presence of Bi, so that Te UPD might shift towards more negative potentials. However, we can reasonably assume that bulk depositions are not significantly affected by the substrate. Hence this UPD peak is very close to the bulk reduction peak, which overlaps with bulk reduction peak and results in the increase of C2.

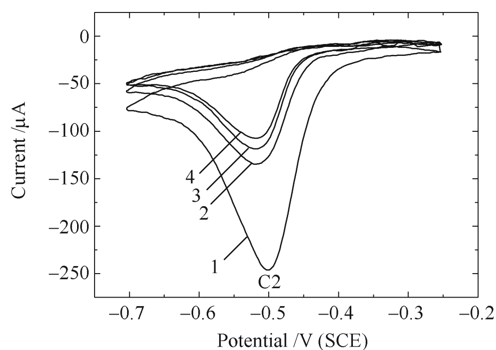

The scanning rate is 10 mV/s.

Fig. 6 Cyclic voltammogram of Te on Bi-covered cold rolled silver surface. The numeral indicates consecutive scans

3.5 Further alternate UPD of bismuth and tellurium

The alternate growth of further UPD of bismuth and tellurium was obtained by keeping the electrode at –0.6 V for 20 s in a Te solution, washing the cell with blank solution, shifting the potential to −1.4 V for 5 s. The Bi blank solution was then introduced. After the Bi blank solution, the Bi solution was pumped in and held quiescent at –0.15 V for 20 s, while Bi UPD layer was deposited, washing the cell and repeating this cycle as many times as desired. EDX quantitative analysis of the 50 cycles sample, obtained by this procedure, gave the 2: 3 stoichiometric ratio of Bi to Te, as expected for the formation of the Bi_2Te_3 compound (Fig. 7). Fig. 8 is an X-ray

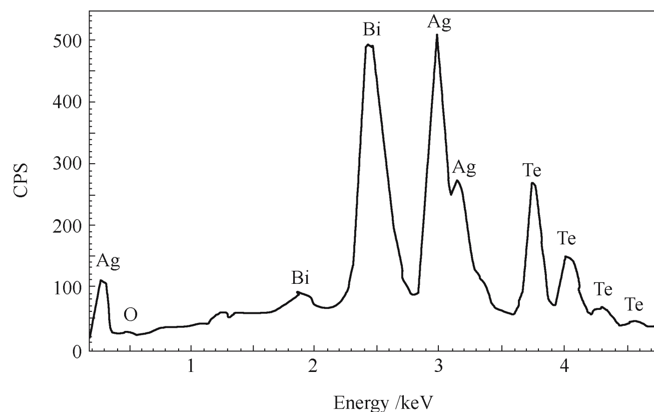

Fig. 7 EDX spectrum of stoichiometric Bi_2Te_3 electrodeposited thin film on cold rolled silver surface

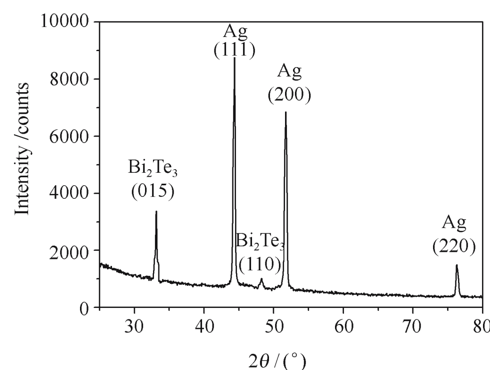

Fig. 8 X-ray pattern of Bi_2Te_3 electrodeposited thin film on Ag

diffraction pattern for a 50-cycle deposit. In the present case, Bi_2Te_3 is a rhombohedral structure compound and the three strong peaks generally occurred at [015], [1010] and [110] plane with the [015] reflection most prominent. As shown in Fig. 8, [015] and [110] reflections are evident, but the [1010] reflection has not been found. Because the X-ray pattern of Bi_2Te_3 [1010] plane is overlapped with the silver [111] plane, so it is reasonable to assume that the Bi_2Te_3 [1010] peak might be covered by the silver [111] peak. It also can be seen that the deposit consists of single phase Bi_2Te_3 compound. There were no indication of elemental Bi and Te; however, peaks of the rhombohedral structure Bi_2Te_3 and Ag substrate were in the in XRD pattern (Fig. 8). In fact, on account of Bi_2Te_3 compound have a larger negative formation enthalpy, and furthermore, larger interface energy exists in the compound that consisted of the single atomic layers owing to the alternate deposition, it will promote the formation of Bi_2Te_3 compound form thermodynamic significance. In addition, there is a direct blend form atomic dimension between Bi and Te atomic layers of alternate deposition, and there is no need for a longer distance diffusion, so that it is also kinetic favorable to form the Bi_2Te_3 compound. As a consequence, forming the Bi_2Te_3 compound spontaneously via the route of alternate deposition of single atomic layer is very favorable in both thermodynamic and kinetic aspect. Further, the obtained deposit has been annealed in short time from Ar flow in 200°C, insured the formation of Bi_2Te_3 compound thin film.

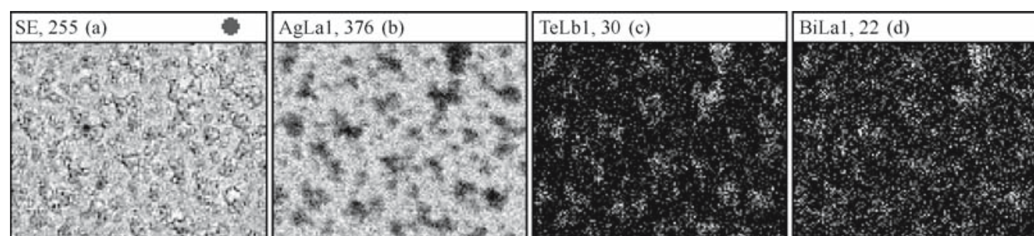

Figure (a) shows back-scattering electron image; Figures (b)–(d) are the map patterns of sample, showing the distribution of silver, tellurium and bismuth respectively.

Fig. 9 EPMA images of the 50 cycles sample

An electron probe microanalyzer (EPMA) attachment was used for Bi and Te elemental analysis. Electron probe microanalysis images of the 50 cycles sample showed a clear two-dimensional worm-like network structure (Fig. 9). Fig. 9(a) shows the back-scattering electron image of the sample. Figs. 9(b), (c), and (d) were the map patterns of sample, showing the distribution of silver, tellurium and bismuth respectively. In Fig. 9(b) the dark areas correspond to Bi_2Te_3 compounds while the bright areas correspond to the silver substrate. In Figs. 9(c) and (d) the bright areas represent Te and Bi elements, respectively. One explanation for the morphology is that it results from the sequential preferential deposition of monolayers of Bi_2Te_3 on nucleation sites, on the surface. Defect sites such as steps and kinks have been found to possess a significant energy of adsorption that may, in some instances, favor the preferential nucleation [16]. In addition, the lattice mismatch of Ag with Bi_2Te_3 is close to 7%, which might result in the formation of an array of dislocations, within the first few deposited Bi_2Te_3 monolayers. Consequently, the preferential nucleation sites might mainly originate from the surface defects of the cold rolled silver substrate and the lattice mismatch of Ag with Bi_2Te_3.

Acknowledgements This work was co-financed by the National Basic Research Program (2004CCA03200), the Chinese National Natural Science Foundation (50401008) and the China Postdoctoral Science Foundation.

References

1. Yang J Y, Aizawa T, Yamamoto A, Ohta T. Effect of processing parameters on thermoelectric properties of p-type $(Bi_2Te_3)_{0.25}(Sb_2Te_3)_{0.75}$ prepared via BMA-HP method. Mater Chem Phys, 2001, 70: 90–94
2. Das V D, Mallik R C. Study of scattering of charge carriers in thin films of $(Bi_{0.25}Sb_{0.75})_2Te_3$ alloy with 2% excess Te. Mater Research Bulletin, 2002, 37: 1961–1971
3. Zou H, Rowe D M, Williams S G. Peltier effect in a co-evaporated Sb_2Te_3(P)-Bi_2Te_3(N) thin film thermocouple. Thin Solid Films, 2002, 408: 270–274
4. Beyer H, Nurnus J, Bottner H, Lambrecht A, Wagner E, Bauer G. High thermoelectric figure of merit ZT in PbTe and Bi_2Te_3-based superlattices by a reduction of the thermal conductivity. Physica E, 2002, 13: 965–968
5. Aboulfarash B, Mzerd A, Giani A, Boulouz A, Pascal-Delannoy F, Foucaran A, Bouer A. Growth of (Bi1-xSbx)2 Te 3 thin films by metal-organic chemical vapour deposition. Mater Chem Phy, 2000, 62: 179–182
6. Yan J W, Wu Q, Shang W H, Mao B W. Electrodeposition of Sb on Au(100) at underpotentials: structural transition involving expansion of the substrate surface. Electrochemistry Communications, 2004, 6: 843–848
7. Tang H, Chen J H, Wang M Y, Nie L H, Kuang Y F, Yao S Z. Controlled synthesis of platinum catalysts on Au nanoparticles and their electrocatalytic property for methanol oxidation. Applied Catalysis A: General, 2004, 275: 43–48
8. Flowers-Jr B H, Wade T L, Garvey J W, Lay M, Happek U, Stickney J L. Atomic layer epitaxy of CdTe using an automated electrochemical thin-layer flow deposition reactor. J Electroanal Chem, 2002, 524: 273–285
9. Fan Y W, Li Y X, Wu C G. Investigations on the ECALE and on the underpotential deposition of Te and Cd elements. J Eastsouth Univ, 1998, 28(1) : 37–42 (in Chinese)
10. Innocenti M, Cattarin S, Cavallini M, Loglio F, Foresti M L. Characterisation of thin films of CdS deposited on Ag(111) by ECALE. A morphological and photoelectrochemical investigation. J Electroanal Chem, 2002, 532: 219–225
11. Pezzatini G, Caporali S, Innocenti M, Foresti M L. Formation of ZnSe on Ag(111) by electrochemical atomic layer epitaxy. J Electroanal Chem, 1999, 475: 164–170
12. Innocenti M, Forni F, Pezzatini G, Raiteri R, Loglio F, Foresti M L. Electrochemical behavior of As on silver single crystals and experimental conditions for InAs growth by ECALE. J Electroanal Chem, 2001, 514: 75–82
13. Vaidyanathan R, Stickney J L, Cox S M, Compton S P, Happek U. Formation of In_2Se_3 thin films and nanostructures using electrochemical atomic layer epitaxy. J Electroanal Chem, 2003, 559: 55–61
14. Vaidyanathan R, Stickney J L, Happek U. Quantum confinement in PbSe thin films electrodeposited by electrochemical atomic layer epitaxy (EC-ALE). Electrochimica Acta, 2004, 49: 1321–1326
15. Forni F, Innocenti M, Pezzatini G, Foresti M L. Electrochemical aspects of CdTe growth on the face (111) of silver by ECALE. Electrochimica Acta, 2000, 45: 3225–3231
16. Colletti L P, Flowers-Jr B H, Stickney J L. Formation of thin films of CdTe, CdSe, and CdS by electrochemical atomic layer epitaxy. J Electrochem Soc, 1998, 145(5): 1442–1449